

Characterization and optimization of the novel TRPM2 antagonist tatM2NX

Cruz-Torres, I.; Backos, D.S.; and Herson, P.S.

*Department of Pharmacology, University of Colorado School of Medicine, Aurora, CO, USA
(I.C.T, P.S.H.)*

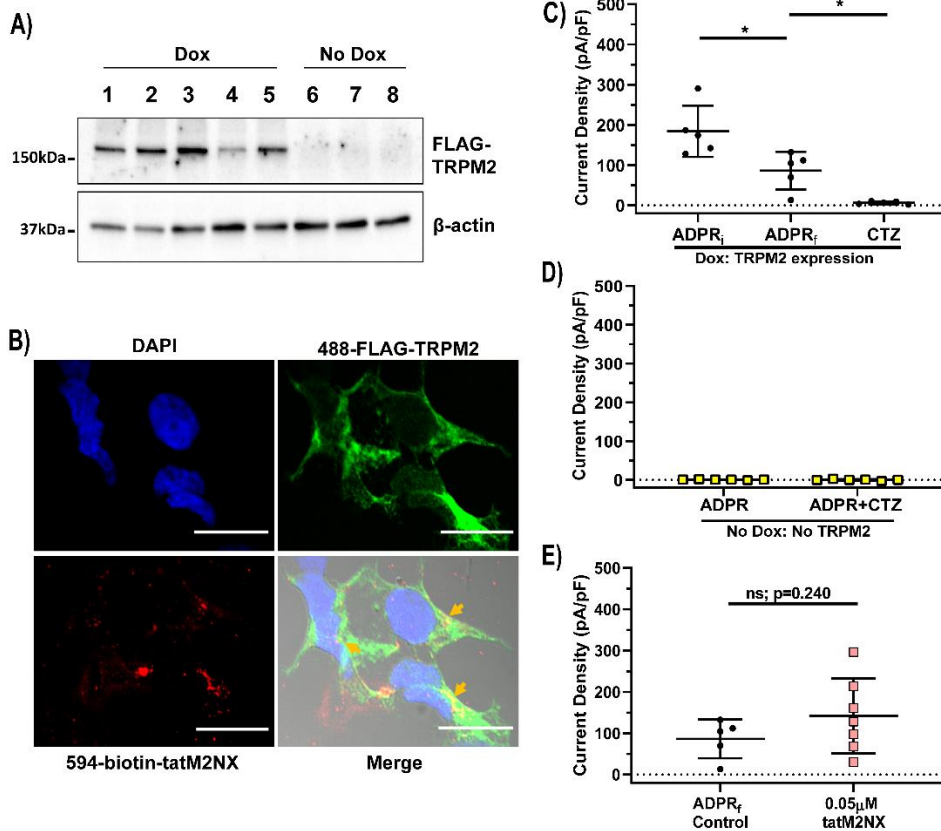
*Department of Pharmaceutical Sciences, University of Colorado Skaggs School of Pharmacy and
Pharmaceutical Sciences, Aurora, CO, USA (D.S.B.)*

*Department of Anesthesiology, University of Colorado School of Medicine, Aurora, CO, USA
(P.S.H.)*

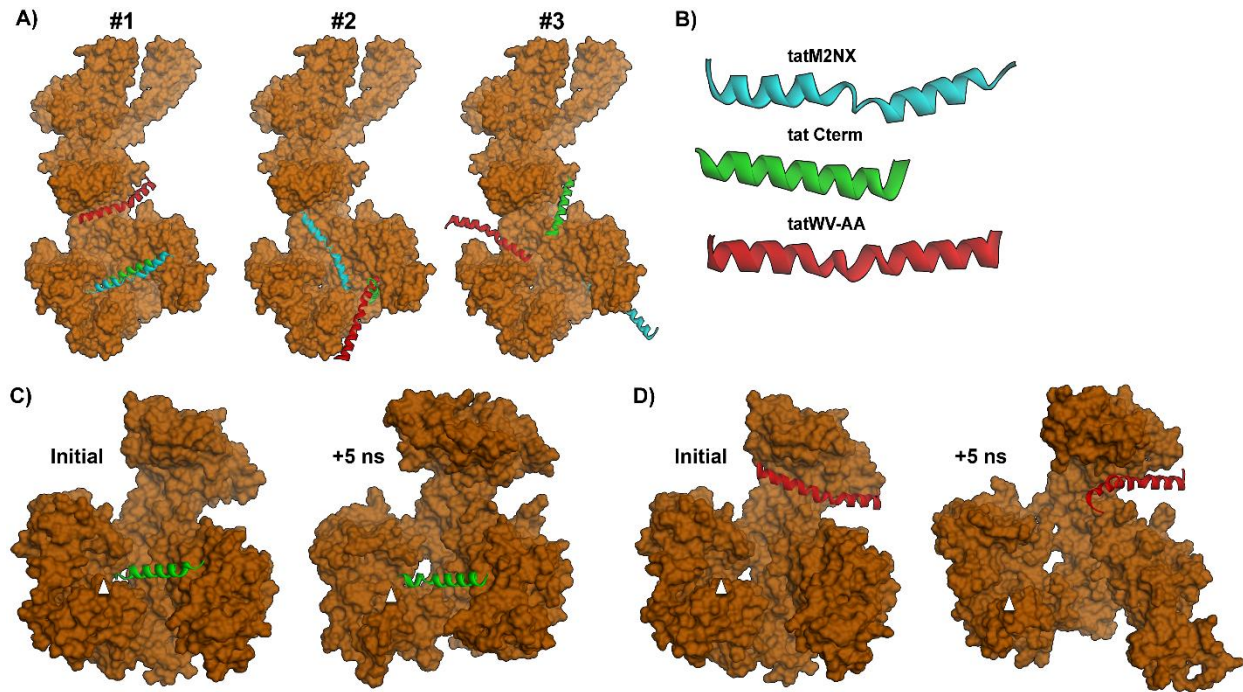
*Neuronal Injury & Plasticity Program, University of Colorado School of Medicine, Aurora, CO,
USA (I.C.T, P.S.H.)*

Corresponding author: Ivelisse Cruz-Torres (ivelisse.cruz-torres@ucdenver.edu), Paco S.
Herson (paco.herson@ucdenver.edu); telephone: 303-724-6628; fax: 303-724-1761

Address: Department of Pharmacology, University of Colorado School of Medicine, Aurora, CO,
USA



Supplemental Figure 1. TRPM2 protein is expressed and functional in doxycycline-inducible HEK293 cells. A) TRPM2 expression detected in HEK293 cells treated with doxycycline (1 μ g/mL) (Dox). No expression in un-treated HEK293 cells (No Dox). B) TRPM2 is expressed in HEK293 cells 16-18h after doxycycline treatment (n=3). Biotin-tatM2NX is found in cells within 1h incubation in the media (yellow arrows). ICC: DAPI (blue), N-terminal FLAG-TRPM2 (green), N-terminal biotin-tagged tatM2NX (red). Scale bar is 25 μ m. C) Rundown (ADPR_i) current density is significantly decreased from ADPR_i current, while CTZ completely inhibits ADPR_i. D) No TRPM2 activity is observed in HEK293 cells in the absence of doxycycline (No Dox). E) ADPR_i compared to 0.05 μ M tatM2NX (ineffective concentration, same group as Figure 2C). All data represented as mean \pm SD and significance established as p < 0.05 for n \geq 5-6 for electrophysiology.

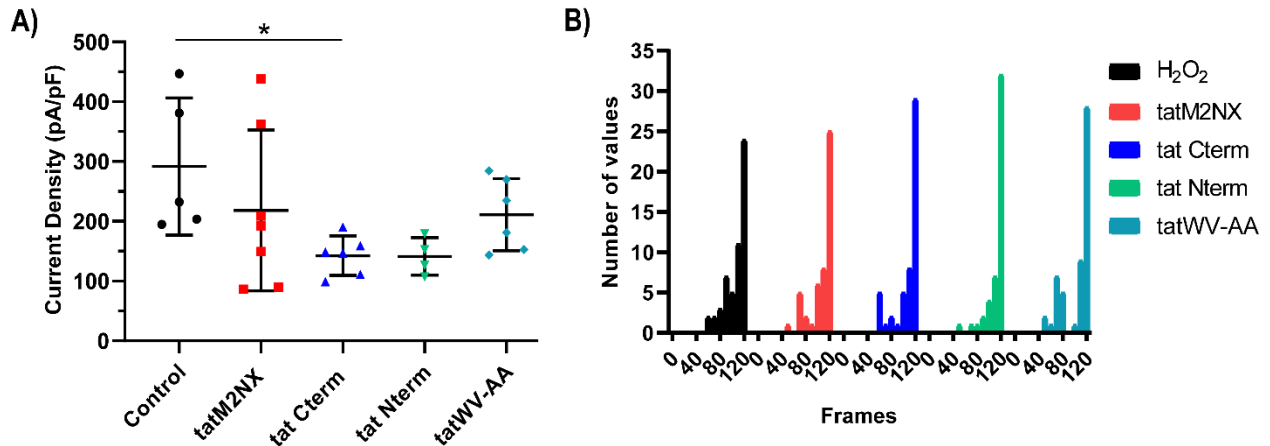


Supplemental Figure 2. Molecular modeling of tat Cterm and tatWV-AA with human TRPM2 channel NUDT9-H domain. A) Top three scoring clusters of tatM2NX (cyan), tat Cterm (green), and tatWV-AA (red) in complex with a single monomer of TRPM2 (orange). B) Predicted secondary structure of tatM2NX (cyan) compared to tat Cterm (green) and tatWV-AA (red) after MD-based refinement. Peptides are oriented N-term (left) to C-term (right). C) Top scoring initial TRPM2-tat Cterm complex (left) and the same complex after 5ns of MD simulation (right). D) Top scoring initial TRPM2-tatWV-AA complex (left) and the same complex after 5ns of MD simulation (right).

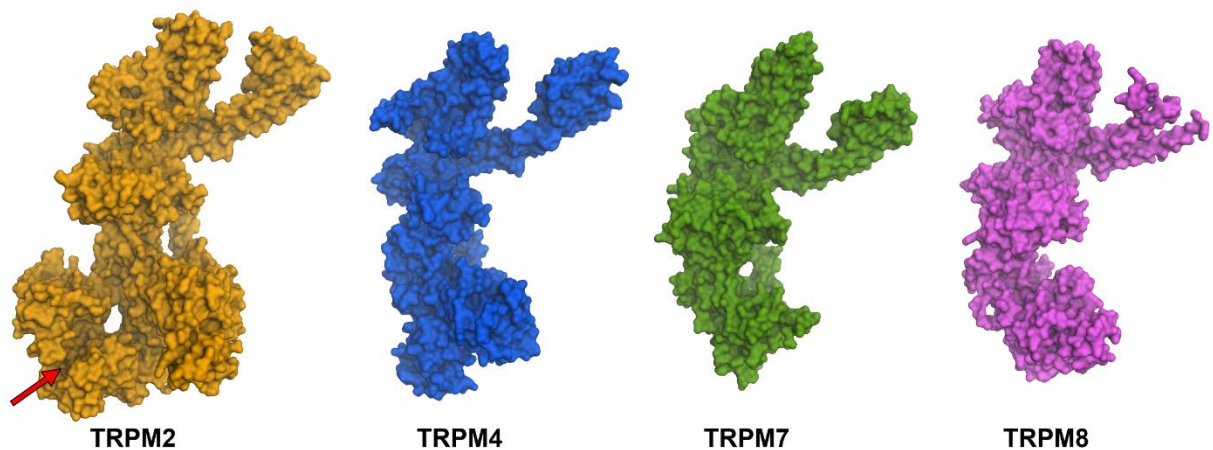
Supplemental Table 1. tat Cterm non-covalent interactions

Interaction (A=TPRM2, E=Peptide)	Interaction Category	Interaction Type
A:ARG1336:HH12 - E:GLU20:OE2	Hydrogen Bond; Electrostatic	Salt Bridge; Attractive Charge
A:ARG1392:HH22 - E:VAL23:O	Hydrogen Bond; Electrostatic	Salt Bridge; Attractive Charge
E:LYS5:HZ2 - A:GLU71:OE1	Hydrogen Bond; Electrostatic	Salt Bridge; Attractive Charge
E:ARG6:HH22 - A:ASP148:OD2	Hydrogen Bond; Electrostatic	Salt Bridge; Attractive Charge
E:ARG9:HH11 - A:ASP148:OD1	Hydrogen Bond; Electrostatic	Salt Bridge; Attractive Charge
A:ARG1336:NH2 - E:GLU20:OE1	Electrostatic	Attractive Charge
A:ARG1392:NH1 - E:VAL23:OXT	Electrostatic	Attractive Charge
A:ARG1433:NH1 - E:VAL23:O	Electrostatic	Attractive Charge
E:TYR1:N - A:GLU71:OE1	Electrostatic	Attractive Charge
E:ARG6:NH1 - A:ASP148:OD2	Electrostatic	Attractive Charge
E:ARG6:NH2 - A:ASP148:OD1	Electrostatic	Attractive Charge
E:ARG6:NH2 - A:ASP289:OD1	Electrostatic	Attractive Charge
E:ARG9:NH1 - A:ASP289:OD1	Electrostatic	Attractive Charge
E:TRP22:HE1 - A:TYR1485:OH	Hydrogen Bond	Conventional Hydrogen Bond
E:LYS5:HE1 - A:GLU71:O	Hydrogen Bond	Carbon Hydrogen Bond
E:ARG9:HD2 - A:ASP148:OD1	Hydrogen Bond	Carbon Hydrogen Bond
E:ARG6:NH2 - A:PHE75	Electrostatic	Pi-Cation
A:LEU1381:C,O;SER1382:N - E:TRP22	Hydrophobic	Amide-Pi Stacked
A:PRO150 - E:LYS5	Hydrophobic	Alkyl
A:HIS118 - E:ARG3	Hydrophobic	Pi-Alkyl
E:TRP22 - A:LEU1381	Hydrophobic	Pi-Alkyl

*3 letter denotes the amino acid; A: TRPM2; E: peptide



Supplemental Figure 3. No changes in ADPR_i current density or frequency distribution in Ca²⁺ fluorescence in the presence of peptides. A) ADPR_i current density was significant ($p=0.0489$, $n=6$) for the peptide tat Cterm. B) Histogram of number of events vs. frames (1 frame=10sec, total 120 frames) in HEK293 cells expressing TRPM2 in response to H₂O₂ in the presence of peptides. All electrophysiology data represented as mean \pm SD, statistical significance at $p<0.05$ for $n\geq 4-10$ (at least 3 experimental days/condition). For Ca²⁺ imaging, histogram was generated from $n\geq 25-53$ (4-6 experimental days).



Supplemental Figure 4. Comparison between the tertiary structures of human TRPM2 (orange), human TRPM4 (blue), mouse TRPM7 (green), and TRPM8 (magenta) (PDB IDs: 6MIX, 6BQR, 5ZX5, and 6NR4, respectively). Arrow indicates the proposed binding site for tatMXN2 within the human ADPR binding pocket, which is not present in the other TRPM family members. This suggests a low potential for tatMXN2 to inhibit other TRPM family members.